Chinese Chemical Letters 31 (2020) 2033–2036

Contents lists available at ScienceDirect

Chinese Chemical Letters

journal homepage: www.elsevier.com/locate/cclet

Communication

Enhanced CO sensing properties of Pd modified ZnO porous nanosheets

Na Luo[a], Bo Zhang[b], Dan Zhang[a], Jiaqiang Xu[a,*]

[a] NEST Lab, Department of Chemistry, Department of Physics, College of Science, Shanghai University, Shanghai 200444, China
[b] School of Materials Science and Engineering, Cultivating Base for Key Laboratory of Environment-friendly Inorganic Materials in University of Henan Province, Henan Polytechnic University, Jiaozuo 454000, China

ARTICLE INFO

Article history:
Received 29 November 2019
Received in revised form 26 December 2019
Accepted 2 January 2020
Available online 3 January 2020

Keywords:
CO sensor
ZnO nanosheet
Pd modifying
Low concentration
Nanocomposite

ABSTRACT

Noble metal is usually used to improve the gas sensing performance of metal oxide semiconductor (MOS) due to its better catalytic properties. In this work, we reported a synthesis of Pd/ZnO nanocomposite by an *in situ* reduction with ascorbic acid (AA). It was found that Pd/ZnO sensor has excellent selectivity to CO and the response of the Pd/ZnO sensor towards 100 ppm CO was as high as 15 (R_a/R_g), obviously higher than that of the pristine ZnO sensor (1.4) when the working temperature is 220 °C. Moreover, the pure ZnO sensor almost has no selectivity to CO, but the Pd/ZnO sensor has excellent selectivity to CO, which may be ascribed to the electronic sensitization of Pd. Our present results demonstrate that the Pd can significantly improve the gas-sensing performance of metal oxide semiconductor and the obtained sensor has great potential in monitoring coal mine gas.

© 2020 Chinese Chemical Society and Institute of Materia Medica, Chinese Academy of Medical Sciences. Published by Elsevier B.V. All rights reserved.

Coalmine gas disaster is the main factor restricting the safety production of a coal mine, especially methane (CH_4) explosion and carbon monoxide (CO) poisoning [1,2]. Hence, the detection of CH_4 or CO under coal mine is essential to prevent the gas concentration exceeds the lower limit of explosion and provide early alarm. Although CH_4 is a main component of coalmine gas [3], the structure of methane is relative stable and it is difficult to detect using MOS sensor [4]. Therefore, by detecting a small amount of CO in the gas, we can also determine the concentration of gas in the mine well. Moreover a low concentration (>35 ppm) of CO in the air may cause headaches and dizziness, and inhalation of a large number of CO molecules (>50 ppm) in a short period of time may lead to human collapse or even death in some cases [5]. Therefore, from the perspective of coal mine safety and human health, it is necessary to develop high standard gas sensors to detect the low concentration of CO.

At present, detection of CO using MOS based gas sensors has attracted widespread attention due to their merits of low cost, easy fabrication, fast response-recover speed, and portability [6–9]. As a typical n-type metal oxide semiconductor, ZnO has attracted much research interest because of their relative excellent gas sensing performance [10–14]. However, single MOS gas sensors aren't content with the actual requirement due to the poor selectivity and low response. Many methods have been used to improve the gas sensing properties of materials, such as surface modification [15], element doping and incorporating another oxide to form composite [16,17]. Especially noble metals doping MOS has been proved to be an effective way to improve gas sensing properties [18–21]. For example, Yonghui Deng *et al.* reported that Au/WO_3 gas sensor possesses enhanced ethanol sensing performance with a good response, high selectivity, and excellent low-concentration detection capability compared with undoped WO_3 sensor [22]. Yuan Zhang *et al.* have reported that ZnO nanowires modified with Pd nanoparticles exhibit a highly enhanced response to H_2S gas, compared to the devices from pure ZnO nanowires [23]. To the best of our knowledge, Pd/ZnO was seldom used to study the sensitization of CO.

Therefore, in this work, a facile two-step route was developed to prepare flower-like ZnO hierarchical structures (HS) that assembled with porous nanosheets (NSs) and then decorated with Pd nanoparticles (NPs) on the surface of ZnO HSs by an in situ reduction of the H_2PdCl_4 with ascorbic acid (AA). It was found that Pd/ZnO sensor exhibited good selectivity for detecting CO at lower temperature (220 °C). The enhanced response and shorter response and recovery times of the Pd/ZnO sensor to CO can be attributed to the electronic sensitization of Pd NPs. Furthermore, the Pd/ZnO sensor is important for detection of coalmine gas concentration in coal mine.

Crystal structure of the pristine ZnO and the ZnO functionalized with Pd were measured by XPS and XRD, respectively. As shown in Fig. 1a, all observed diffraction peaks of the products are matched well with the tetragonal ZnO structure. The complete XPS spectra

* Corresponding author.
E-mail address: xujiaqiang@shu.edu.cn (J. Xu).

https://doi.org/10.1016/j.cclet.2020.01.002
1001-8417/© 2020 Chinese Chemical Society and Institute of Materia Medica, Chinese Academy of Medical Sciences. Published by Elsevier B.V. All rights reserved.

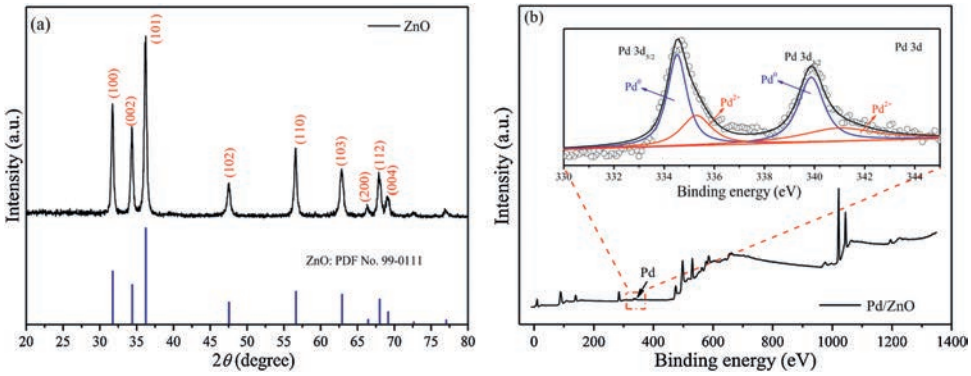

Fig. 1. (a) XRD patterns of ZnO, (b) XPS result of survey spectrum of Pd/ZnO; (inset pattern) banding energy spectrums of Pd 3d.

of Pd/ZnO are shown in Fig. 1b, which confirms the presence of Pd elements in samples. Moreover, the Pd high-resolution was displayed in inset pattern. The spinorbit coupling energy gap between Pd $3d_{5/2}$ and Pd $3d_{3/2}$ is 5.4 eV and the asymmetrical Pd $3d_{5/2}$ peak could be decomposed into two peaks with BE at ~334.7 and ~340.0 eV, which could be attributed to Pd^0 and Pd^{2+} [3]. PdO can significantly affect the sensing performance of MOS by electronic sensitization during this reaction (Pd ⇌ PdO) [24].

Figs. 2a and b show the typical FESEM image of the prepared ZnO. It is interesting to observe that the obtained ZnO product perfectly inherits the flower-like morphology. The FESEM images of Pd/ZnO sample (Figs. 2c and d) are similar with the FESEM images of ZnO, indicating that the introduction of Pd has almost no influence on the morphology of the ZnO. Pd NPs-decorated mesoporous ZnO HS can be further synthesized by using TEM. The low-magnification TEM images taken from Pd/ZnO (Fig. 2e) clearly show the porous structure of the nanosheets. From high-resolution TEM images (Fig. 2f), the Pd NPs were approximate size and uniform dispersion on the ZnO NSs. Fig. 2g displays the selective area electron diffraction (SAED) pattern recorded from Fig. 2e. The clear and sharp diffraction rings reveal the good crystallinity of the samples and the diffraction rings from inner to outer can be indexed as two definite phases, including the (100), (002), (101), (102) and (110) planes of ZnO (JCPDS No. 99-0111) and the (111) planes of Pd (JCPDS No. 87-0637), once again demonstrating that the Pd has been successfully loaded on ZnO NSs. In the HRTEM image (Fig. 2h), the measured distances between adjacent lattice fringes are 0.2285 nm and 0.260 nm, which can be ascribed to (111) plane of Pd (JCPDS No.87-0637) and (002) plane of ZnO (JCPDS No. 99-0111), respectively. In addition, the interlaced lattice fringes between Pd and ZnO indicate the formation of Pd/ZnO junction on the porous nanosheets.

In this study, we explore their potential applicability in CO gas sensing. Since the working temperature can exert severe impacts on the gas sensing properties of the materials [25], the responses of the Pd/ZnO sensor to CH_4, CO, H_2S were first tested at different working temperatures to find their optimum working temperature (OWT). As shown in Fig. 3a, the Pd/ZnO sensor exhibit an "increase-maximum-decrease" trend in response to CO with the working temperature increasing from 150 °C to 240 °C, and the response can reach a maximum when the OWT is 220 °C. In addition, the response value of the Pd/ZnO sensor to 100 ppm CO (14.8) is much higher than that to 1000 ppm CH_4 (1.15) and 100 ppm H_2S (1.03), demonstrating that Pd/ZnO sensor has excellent selectivity to CO. As shown in Fig. 3b, the responses of Pd/ZnO sensor to all tested gases are obviously higher than the ZnO but the response of ZnO sensor to different gas is approximately same. Moreover the response of Pd/ZnO sensor to CO is about 14.8, which is 17 times as much as the ZnO sensor. The improvement of the selectivity and the enhancement of sensing responses can be attributed to the comprehensive effect of catalytic effect and the sensitization effect of Pd NPs.

The dynamic response-recover curves of the Pd/ZnO and ZnO sensors towards different concentrations of CO were tested. In the

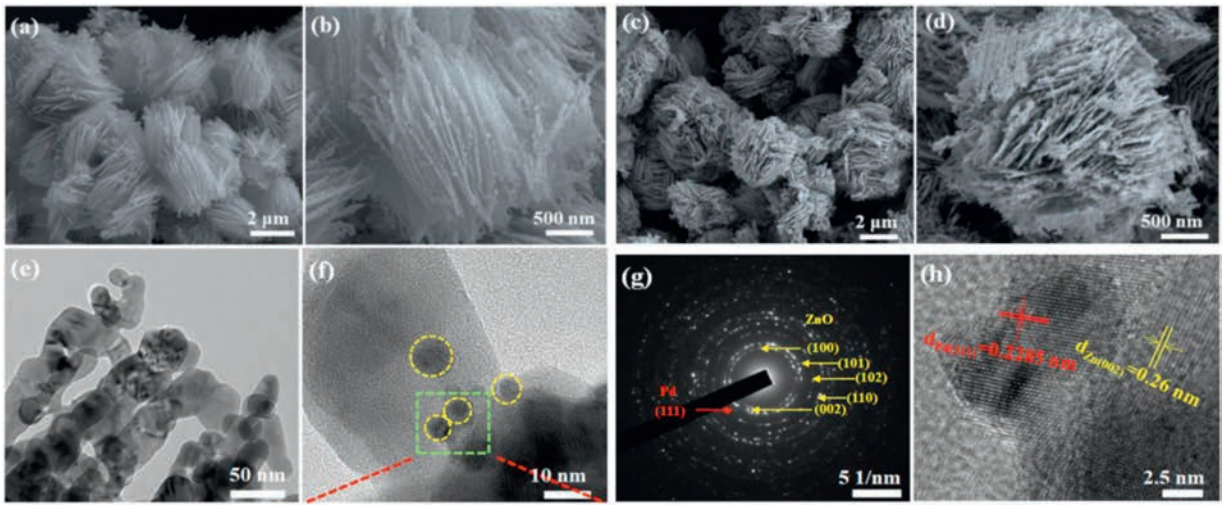

Fig. 2. FESEM images of the prepared (a, b) ZnO and (c, d) Pd/ZnO hierarchical structures. (e, f) TEM image of the Pd/ZnO porous nanosheet. (g) SAED pattern and (h) HRTEM images corresponding to the areas denoted in (f).

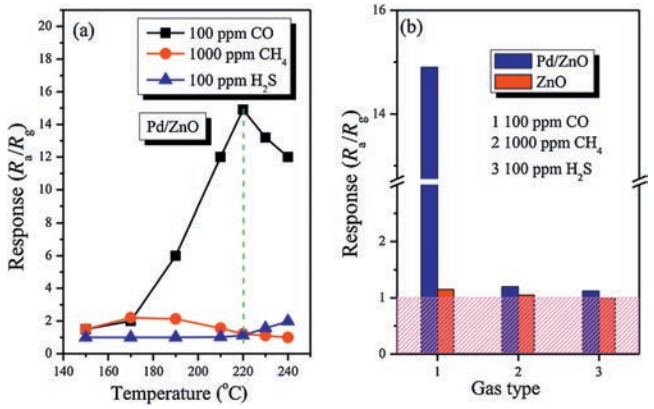

Fig. 3. (a) Response versus operating temperature of Pd/ZnO sensors to different gases, (b) response of Pd/ZnO and ZnO sensor to different gases at 220 °C.

CO atmosphere, the obvious differences between the ZnO and Pd/ZnO sensors are the level of resistance change and the response time. As shown in Figs. 4a and b, once exposed to different concentrations of CO, the Pd/ZnO sensor can give a more obvious response and the response increase gradually with the concentration increasing from 20 ppm to 180 ppm, demonstrating the Pd/ZnO sensor has better response ability to CO. However, in the CH_4 or H_2S atmosphere, the response ability of Pd/ZnO sensor to tested gas is similar to ZnO sensor (Fig. S1 in Supporting information). As shown in Fig. S2 (Supporting information), the response times of Pd/ZnO and ZnO sensors to 100 ppm CO were determined to be 100 s and 350 s, respectively, and the recovery time of Pd/ZnO is only 255 s, much shorter than that of ZnO (425 s). While, the response of the Pd/ZnO sensors to different concentrations of CO are obviously higher than that of the ZnO sensor as shown in Figs. 4c and d, which revealing the positive effect of Pd on the gas sensing properties of ZnO.

The CO sensing properties of the present Pd/ZnO were also compared with other materials reported in literatures. As shown in Table S1 (Supporting information), the Pd/ZnO can give comparable response, demonstrating its good CO sensing property at relatively low working temperature. The reversible cycles of the response curve in Fig. 4e reveal a stable and reliable operation for CO sensing of the sensors based on Pd/ZnO. In a period of 50 days, the sensor gives almost the same response, further confirming reliable repeatability of the Pd/ZnO sensor (Fig. 4f).

In this mechanism, the sensor performance strongly depends on Pd obviously. Based on the above analysis of gas sensing characteristic, the improved CO sensing performance of the Pd/ZnO sensor should be attributed to catalysis and electronic sensitization of Pd.

At first, the gas-sensing mechanism schematic diagrams of ZnO sensor are shown in Figs. 5a and b. The main carrier of n-type semiconductor is the electrons, which play a vital effect on electron properties of metal oxide semiconductor. As shown in Fig. 5a, the oxygen molecules can adsorbed on the surface of ZnO and then trap electrons from the conduction band and form the oxygen ions species when the ZnO sensor are exposed to air [26]. Due to the redox reaction between CO and oxygen ions in the CO atmosphere, the electrons will be released to the conduction band of ZnO. The thickness of the electrons depletion layer (EDL) will becomes thinner and the resistance of the sample will be decreased (Fig. 5b).

The sensitization mechanism of Pd mainly includes the following two aspects, catalysis and electronic sensitization. Firstly, the Pd nanoparticles can catalytic the dissociation of the oxygen molecule and then O^- diffuse to the surface of the metal oxide [27], and the content of adsorbed oxygen of ZnO surface will increases from 33.0% to 47.1% (Fig. 5c and Fig. S4 in Supporting information). Moreover, Pd nanoparticles can catalyze the reaction between CO and O^-, allowing more electrons to be released back into the conduction band of ZnO [28]. Secondly, the electronic sensitization of Pd also plays an important role in improving the response. Because of the different work function of Pd (5.6 eV) [29] and ZnO (5.2 eV) [30], the electrons in ZnO will flow to Pd, resulting in that the thickness of EDL at the interface between Pd and ZnO decrease (Fig. 5c), which can be proved by Fig. S3 (Supporting information). From this figure it can be clearly seen that the R_a value of Pd/ZnO is about 13.2 MΩ, which is higher than that of ZnO (77 kΩ), proving that Pd/ZnO has a thinner EDL. Generally

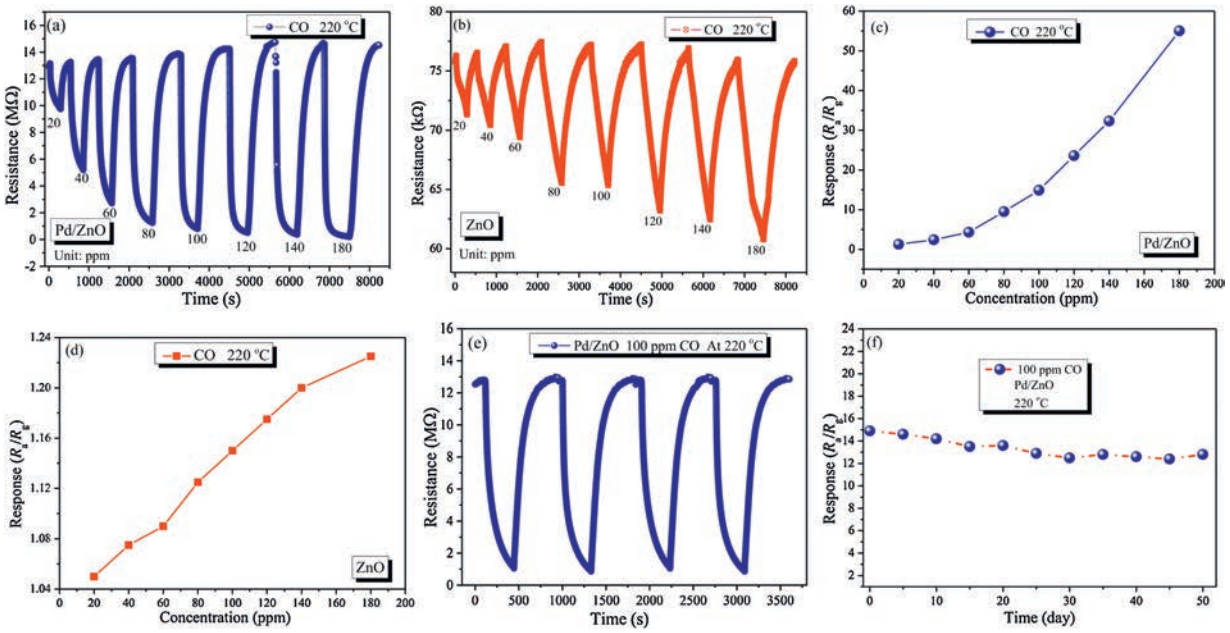

Fig. 4. Dynamic response-recover curves of (a) the Pd/ZnO and (b) ZnO sensors to different concentrations of CO at 220 °C. (c, d) The linear relationship between response and concentration within 20–180 ppm. (e) Repeatability and (f) stability measurements of the Pd/ZnO sensor.

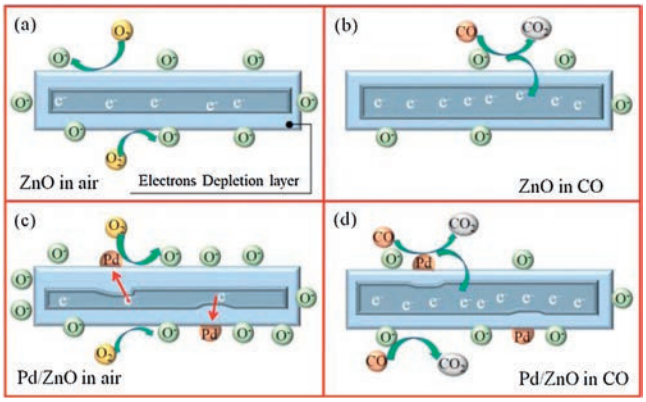

Fig. 5. The gas-sensing schematic diagram of ZnO exposed to (a) air and (b) CO, Pd/ZnO exposed to (c) air and (d) CO.

speaking, the high R_a value for an n-type MOS sensor is advantageous to achieve higher response, because the response was defined as R_a/R_g. Fig. 5c shows that when the sensor is exposed CO ambience, the redox reaction will occur on the surface of ZnO porous nanosheets. CO molecules react with chemisorbed oxygen anions to form CO_2, which can be demonstrated by DRIFTS (Fig. S4). After which the electrons captured by oxygen anions will be released back to ZnO (Fig. 5d), leading to the lower sensor resistance (R_g). Therefore, Pd/ZnO sensor exhibits a higher response to CO in comparison with pristine ZnO sensor.

In summary, the Pd modified ZnO NSs have been synthesized by the in situ reduction method. The sensor based on Pd/ZnO demonstrated better selectivity to CO compared with pristine ZnO sensor. Moreover, Pd modified ZnO samples showed higher response, shorter response and recovery time under their optimum working temperature (220 °C). The improvement of the gas sensing performance of ZnO can be attributed to the catalysis and electron sensitization of Pd, which has a great potential in monitoring coal mine gas.

Declaration of competing interest

The authors declare that they have no known competing financial interests or personal relationships that could have appeared to influence the work reported in this paper.

Acknowledgments

The authors acknowledge the support of the National Natural Science Foundation of China (Nos. U1704255 and 61671284) and the Shanghai Committee of Science and Technology, China (No. 17010500500).

Appendix A. Supplementary data

Supplementary material related to this article can be found, in the online version, at doi:https://doi.org/10.1016/j.cclet.2020.01.002.

References

[1] K. Bunpang, A. Wisitsoraat, A. Tuantranont, et al., Sens. Actuator. B -Chem. 291 (2019) 177–191.
[2] F. Fernández-Sánchez, I. Fernández, R. Steiger, et al., Adv. Funct. Mater. 17 (2007) 1188–1198.
[3] G. Li, X. Wang, L. Yan, et al., ACS Appl. Mater. Interfaces 11 (2019) 26116–26126.
[4] B.K. Min, S.D. Choi, Sens. Actuator. B -Chem. 108 (2005) 119–124.
[5] S.R. Ryu, S.D. Ram, H.D. Cho, et al., Nanoscale 7 (2015) 11115–11122.
[6] T. Krishnakumar, R. Jayaprakash, N. Pinna, et al., Sens. Actuator. B -Chem. 143 (2009) 198–204.
[7] M. Hjiri, L. El Mir, S.G. Leonardi, et al., Sens. Actuator. B -Chem. 196 (2014) 413–420.
[8] Z. Xue, Z. Cheng, J. Xu, et al., ACS Appl. Mater. Interfaces 9 (2017) 41559–41567.
[9] R. Chen, Y. Hu, Z. Shen, et al., ACS Appl. Mater. Interfaces 8 (2016) 2591–2599.
[10] A. Tamvakos, K. Korir, D. Tamvakos, et al., ACS Sens. 1 (2016) 406–412.
[11] Y. Li, D.L. Li, J.C. Liu, Chin. Chem. Lett. 26 (2015) 304–308.
[12] C. Li, Z.S. Yu, S.M. Fang, et al., Chin. Chem. Lett. 19 (2008) 599–603.
[13] L. Chen, J. Cui, X. Sheng, et al., ACS Sens. 2 (2017) 897–902.
[14] R. Chen, Y. Hu, Z. Shen, et al., ACS Appl. Mater. Interfaces 8 (2016) 2591–2599.
[15] A. Montazeri, F. Jamali-Sheini, Sens. Actuator. B -Chem. 242 (2016) 778–391.
[16] A. Gaiardo, B. Fabbri, A. Giberti, et al., Sens. Actuator B -Chem. 237 (2016) 1085–1094.
[17] W. Li, H. Xu, T. Zhai, et al., Sens. Actuator. B -Chem. 253 (2017) 97–107.
[18] J. Liang, J. Liu, N. Li, W. Li, J. Alloys Compd. 671 (2016) 283–290.
[19] J. Zhang, X. Liu, S. Wu, B. Cao, S. Zheng, Sens. Actuator. B -Chem. 169 (2012) 61–66.
[20] H. Cai, H. Liu, T. Ni, et al., Front. Chem. 7 (2019) 843–856.
[21] X. Xiao, Y. Zou, Y. Ren, et al., Small 15 (2019)1904240.
[22] Y. Zhang, Q. Xiang, J. Xu, et al., J. Mater. Chem. 19 (2009) 4701–4706.
[23] N. Yamazoe, G. Sakai, K. Shimanoe, Catal. Surv. Asia 7 (2003) 63–75.
[24] D. Wang, L. Tian, H. Li, K. Wan, et al., ACS Appl. Mater. Interfaces 11 (2019) 12808–12818.
[25] Y. Zhu, Y. Zhao, J. Ma, et al., J. Am. Chem. Soc. 139 (2017) 10365–10373.
[26] H.G. Moon, Y. Jung, D. Jun, et al., ACS Sens. 3 (2018) 661–669.
[27] A. Merenda, M. Weber, M. Bechelany, et al., Appl. Surf. Sci. 483 (2019) 219–230.
[28] G. Li, Z. Cheng, Q. Xiang, et al., Sens. Actuator. B -Chem. 283 (2019) 590–601.
[29] Y. Li, N. Luo, G. Sun, et al., Sens. Actuator. B -Chem. 287 (2019) 199–208.